Chemical Science

Accepted Manuscript

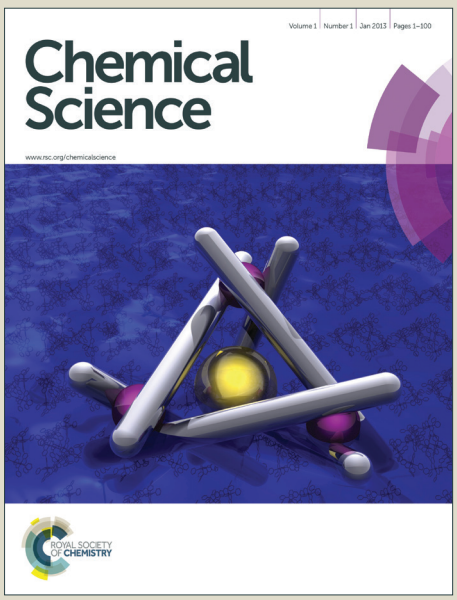

ROYAL SOCIETY OF CHEMISTRY

www.rsc.org/chemicalscience

Visualizing Tilted Binding and Precession of Diatomic NO Adsorbed to Co-porphyrin on Au(111) using Scanning Tunneling Microscopy

Howon Kim[†], Yun Hee Chang[‡], Soon-Hyeong Lee[†], Soobin Lim[†], Seung-Kyun Noh[†], Yong-Hyun Kim[,‡,#] and Se-Jong Kahng[*,†]*

[†]Department of Physics, Korea University, 145 Anam-ro, Seongbuk-gu, Seoul 136-713, Republic of Korea,

[‡]Graduate School of Nanoscience and Technology, KAIST, 291 Daehak-ro, Yuseong-gu, Daejeon 305-701, Republic of Korea

[#]Center for Nanomaterials and Chemical Reactions, Institute for Basic Science (IBS), 291 Daehak-ro, Yuseong-gu, Daejeon 305-701, Republic of Korea

(e-mail : yong.hyun.kim@kaist.ac.kr; sjkahng@korea.ac.kr)

KEYWORDS : Co-porphyrin, nitric oxides, scanning tunneling microscopy, density functional theory

ABSTRACT : The axial bindings of diatomic molecules to metalloporphyrins play key roles in dynamic processes of biological functions. The basic knowledge of binding structures of NO adsorbed to Co-porphyrin remains unsettled; recent scanning tunneling microscopy showed center protrusion images, while X-ray diffraction and nuclear magnetic resonance spectroscopy revealed tilted binding structures of NO. Here we report high-resolution scanning tunneling microscopy images of NO adsorbed to Co-porphyrins which show perfect agreement with the latter. Upon NO exposure, three-lobed structures of Co-porphyrins were transformed to bright ring shapes on Au(111). With the help of density functional theory calculations, we reproduce the bright ring shapes in the simulated scanning tunneling microscopy image by considering tilted binding and precession motion of NO. Thus, our study directly visualizes the NO ligand of the NO-Co-porphyrin nitrosyl complexes that is tilted away from the axis normal to the porphyrin plane, and is being under precession.

Introduction

The axial bindings of diatomic molecules such as nitric oxide (NO) to metalloporphyrins are involved in dynamic processes of biological functions including neurotransmission[1-5] and dilation of blood vessels[6-9]. These binding reactions provide the ways to control molecular electronic-states and spin-configurations of metalloporphyrin systems that can be used in bio-sensing[2, 10] and spintronic applications[1, 11-14]. In the binding reactions, a four coordinated metal at the center of metallophorphyrins transforms to five and six coordinated one [15-18]. The geometry of the five and six coordinated metal structures with NO and other diatomic molecules was early predicted by Enemark and Feltham[19], and has been actively studied for the last four decades[20-25]. An important theoretical prediction was that, in the case of Co tetraphenylporphyrin (CoTPP) and NO, the angle of Co-N-O was about 120°. Thus the NO ligand attached to Co atom should be significantly tilted away from the axis normal to the porphyrin plane. The tilting prediction was examined by X-ray diffraction (XRD) experiments performed on molecular crystals of NO-CoTPP which were solidified after solution-phase reactions of NO and CoTPP [22, 26-28]. The Co-N-O angles found in XRD experiments were within a range between 119.6° and 135.2°. In addition, based on nuclear magnetic resonance (NMR) experiments, it was argued that the NO was not only tilted and but also swing or spinning with finite thermal excitation[29]. In contrast to these backgrounds, recent scanning tunneling microscopy (STM) experiments show no direct indication of a tilted binding, mostly showing center-protrusion images in NO-CoTPP on Ag(111)[30-32]. In the STM experiments, a CoTPP monolayer was prepared and exposed to NO gas in a vacuum condition, different from bulk crystals reacted in solution phases. It became questionable if metal-supported molecules should

have different behaviours from bulk-crystalline molecules due to dimensional, substrate, or reaction-condition (i.e. solution v.s. vacuum) effect.

In this paper, we report on the binding structures of NO-CoTPP on Au(111) studied using STM and density functional theory (DFT) calculations. It has been known that Au(111) has weaker substrate effect than others including Ag(111)[33, 34]. After exposure to NO gas, our STM data clearly showed that CoTPP's three-lobed structures were replaced by bright ring structures. This can be explained, with the help of DFT calculations, by the formation of NO-CoTPP complexes where tilting and precession-motion occur. The tilt angle was estimated to be 122.8°. Our experiment is the first direct observation of tilting and precession in NO-CoTPP at the single molecule level.

Experiments

The growth experiments were performed in-situ using our home built STM system operating at 80 K with a base pressure of 1×10^{-10} Torr. The Au(111) surface was prepared using commercially available Au thin film (200 nm thick, PHASIS, Switzerland) on mica that was exposed to several cycles of Ne-ion sputtering and annealing at 800 K. The surface cleanliness of the Au(111) was observed by checking the typical herringbone structures and atomic lattices using STM images. A mixture of commercially available CoTPP (Porphyrin Systems, Germany) and H_2TPP (Sigma Aldrich, USA) was outgassed in a vacuum for several hours and then deposited on the Au(111) at submonolayer coverages by thermal evaporation using an alumina-coated evaporator. NO gas (99.95 %) was introduced using a stainless steel tube (3 mm diameter) through a precision leak valve. A vibration spectroscopy, Fourier transform infra-red

(FTIR) spectroscopy was performed *ex-situ* for CoTPP on the Au(111) with and without NO exposure. Thermo Mattson Nicolet 5700 spectrometer was used in to measure FTIR spectra for thick layers of CoTPP (> 200 nm).

Results and discussions

When a mixture of CoTPP and H_2TPP (about 50:50) was deposited on Au(111), the two different molecules randomly occupied sites in the square grids of molecular islands [see Fig. S1]. Both molecules have four bright dots at the locations of the phenyl groups which have dihedral rotations about the C-C bonds connecting the phenyls to macrocycles. The macrocycles of molecules show either a three-lobed or a dark-ring structure. The molecules with a three-lobed structure are CoTPP that shows bright center due to Co atom at -0.5 eV [30-32, 35-39]. At +0.6 eV, the CoTPP shows a single-lobe structure with the bright center in agreement with previous reports[39, 40]. The molecules with a dark ring are H_2TPP that shows center depression due to an absent electronic state[31, 35-37]. The two-fold symmetry, instead of four-fold, of both molecules was explained by saddle-type deformation made by adsorption on metal substrates. These molecular islands were exposed to NO gas at 80 K with the STM tip retracted. Figures 1(a) and (b) show the STM images obtained after 900 L exposure of NO gas. In addition to the two molecules observed before NO exposure, the molecules with bright ring shape appear [See Fig. S3]. In a better resolution image and height profiles in Fig. 1(c) and (d), respectively, we can see the bright rings have the height variation of 0.11 nm and a peak-to-peak distance of 0.25 nm. When the image of a molecule was further zoomed as shown in Fig. 2(a), the ring looked like a rectangular ring with four lobes. The lateral distances between the centers of two lobes were 0.18 nm, as revealed in the height profiles of Fig. 2(b). Four lobes of a square located in the lines

connecting Co and the centers of phenyl rings. We assigned the bright rings to be structures of the NO-CoTPP nitrosyl complex, which will be justified later by our calculation results.

We observed that NO exposure did not affect the shapes of the H_2TPPs, implying that the spontaneous NO binding is highly selective. The bright rings of NO-CoTPP and the dark rings of H_2TPP, in our experiments on Au(111), are never alike in the sense that both the heights (brightnesses) and sizes of the rings as clearly distinct as shown in Fig. 1(c). The height difference between the two structures was about 0.2 nm. The lateral size of dark rings of H_2TPP was about 0.8 nm, more than three times that of the bright rings of NO-CoTPP. In contrast, it was reported that on Ag(111) the shape of NO-CoTPP was very similar to that of H_2TPP in the STM images obtained with a metal terminated tip with low spatial resolution[31]. Using molecule-terminated STM tip, it was reported that NO-CoTPP showed center-protrusion images on Ag(111), but DFT calculation results predicted tilted binding of NO to CoTPP on Ag(111)[31, 32]. STM images in Figs.1 and 2 were obtained without unwanted tip effect. STM images obtained with typical tip effects such as double tip and asymmetric tip are provided in Supporting Information [See Fig. S4]. To make sure the electronic relevancy of our tip, we repeatedly performed scanning tunneling spectroscopy at bare Au(111) regions before and after the NO exposure, confirming that well-known surface state of Au(111) was resolved at -0.48 eV.

To understand the bright square ring structures observed in our experiments, we performed DFT calculations regarding NO-adsorbed Co-porphyrin (CoP) and CoTPP on Au(111) using the Vienna Ab Initio Simulation Package (VASP)[41], in which Kohn-Sham wave functions are expanded by a series of plane waves with a kinetic energy cut-off of 400 eV. The projector-augmented wave (PAW) potentials[42] and the exchange-correlation functional of the Perdew-Burke-Ernzerhof (PBE)[43] were used to calculate electron-ion and electron-electron interactions,

respectively. We used an Au(111) slab model with a p(6×6) surface unit cell (36 surface Au atoms) and three atomic layers. It is widely known that the PBE functional is insufficient for weak dispersion interactions[44], so we also used the dispersion corrected DFT-D method to account for the van der Waals interactions between the CoP (or CoTPP) and Au(111)[45]. The constant-current STM images are simulated within the Tersoff-Hamann approximation[46].

Figure 3(a) and (b) show the vertical and tilted binding structures of NO adsorbed to CoP, respectively. Both structures are DFT-optimized on Au(111), although Au atoms were not drawn for visual clarity. The vertical stucture has C_{4v} symmetry with the a binding energy of 0.76 eV, but is an unstable equilibrium point in the potential energy surface against tilting distortion. Therefore, the tilted binding structure is the most stable configuration with the binding energy of 1.81 eV. The calculated Co-N-O angle is 122.8°, which is consistent with previous theoretical and experimental reports[16, 19, 22, 23, 26-28]. When the NO-CoP is viewed from the top, the N and O-atoms locate at the extended line of C-C bonds that connect the phenyls to macrocycles. From molecular-orbital analysis, we found that the tilted geometry stemmed from strong orbital hybridization between the Co-d_z^2 and NO-ppπ^* states. The coupling mechanism and tilted diatomic geometry are similar to the O_2 adsorption seen in the Heme or Fe-porphyrin molecule[47]. Namely, tilting geometry provides far more efficient ways to maximize orbital overlap between d_z^2 and ppπ^* than vertical geometry.

Due to the symmetry of the CoP, the adsorbed NO molecule could have a precession motion. To see this, we performed a Nudged Elastic Band (NEB)[48] calculation about the 90°-precession motion of the tilted NO molecule, as shown in Fig. 3(c). An energy barrier of 40 meV was found, when the tilted NO is directed to the Co-N bonds. This energy barrier is small enough to allow a

fast precession motion of the NO molecule even in cryogenic temperatures as low as 80 K. The precession frequency can be estimated by $\omega = \omega_0 \exp(-E_a/k_BT)$, where E_a is the energy barrier, k_B is the Boltzmann constant, T is temperature, and ω_0 is the attempting frequency or vibration frequency. Using $\omega_0 = 4\times10^{13}$ s^{-1}, E_a = 40 meV, and T = 80 K, the precession frequency is of the order of 10^{10} s^{-1}, i.e., 10 rotations per 1 ns. In addition, because the electron tunneling voltage is -0.6 eV, the electronic energy is large enough to perturb the precession motion. This fast precession corresponds to the swinging or spinning motions observed in a previous NMR experiment[29].

We simulated a constant-current STM image for NO-CoP on an Au(111) substrate without and with precession motion. Precession motion was considered as hopping around four equivalent configurations. The simulation bias voltage is -0.6 eV in the filled state image. For a fixed NO molecule, the oxygen terminal gives a bright protrusion that has a node between the N and O atoms as shown in Fig. 3(d). By making precession of the NO molecule on top of the CoP, we could obtain a bright square ring in the simulated STM image, as shown in Fig. 3(e). In order to extract quantitative information, height profiles of the square ring at a simulated constant current were obtained, as shown in Fig. 3(f). The height profiles again clearly show the square ring feature, corresponding to the lateral size of about 0.18 nm. The large lateral size, compared to 0.14 nm from the NO bond length and tilted angle, can be attributed to the spread of the molecular orbitals.

The binding energy and titled configuration of the NO molecule adsorbed to CoP was not significantly affected by considering the Au(111) substrate, CoTPP molecule, the van der Waals interaction correction, as summarized in Table 1. Thus, we believe that the precession motion of

NO occurs regardless of such variations. To be more realistic, we also performed the STM image simulations for NO-CoTPP on Au(111) substrate. We used saddle conformations for the CoTPP on Au(111). Figure 4 shows (a) the tilted binding structures of NO-CoTPP optimized by DFT calculations and (b) STM images with precession motion. Although the details of bright rings in NO-CoP and NO-CoTPP vary --the former is a square and the latter is a rectangular ring--, both cases clearly reproduce the key features of a bright ring, a dark center and four lobes, in agreement with experimental STM images. Thus we conclude that the observed bright rings are the results of precession motion or hopping of a tilted NO molecule between four stable sites on the CoTPP. Tilted binding of CO without precession on Fe and Pd adatoms on metal (110) surfaces was reported using STM by the contribution of d_{xz} orbitals, different from NO-CoTPP systems[49-52].

We double-checked that the chemical identity of molecules adsorbed to CoTPP with a vibration spectroscopy, Fourier transform infra-red (FTIR) spectroscopy. Figure 5 shows the two FTIR spectra obtained from CoTPP with and without NO exposure. Both spectra clearly reproduce the well-established vibration modes of CoTPP, 702, 754, 806, 1006, 1073, 1351, and 1440 cm^{-1}. The spectrum obtained from CoTPP with NO exposure shows two additional modes at 1283 and 1680 cm^{-1}. The latter is the stretching mode of NO[53-55], and the former is the symmetric mode of NO_2[56]. Because we could not find any trace of NO_2 from our mass spectroscopy experiment performed *in-situ* [See supporting information Fig. S5], we believed that the NO_2 was formed when the NO-CoTPP was exposed to air for FTIR measurements. It was reported that addition of O_2 into NO-FeTPP lead to the appearance of NO_2 vibration modes by the reaction between NO and O_2[54]. Therefore, we confirmed that the molecules adsorbed to CoTPP were NO. When a NO molecule is adsorbed to Fe and Mn-porphyrin in upright-like

geometry, with the metal-N-O angle close to 180°, the stretching mode of NO appears near that of gas phase NO, 1875 cm^{-1}[18]. On the other hand, NO molecules with tilted binding geometry tend to have the reduced stretching modes around 1670 cm^{-1}[18]. Thus the observed stretching mode 1680 cm^{-1} in our experiments is another signature of tilted binding, in agreement with our STM and DFT calculation results.

In summary, we observed a structural transformation of CoTPP from a three-lobed to a bright square ring structure upon NO exposure using STM. With DFT calculations, the bright square ring structures were explained by the fast precession motion of a tilted NO molecule adsorbed onto Co-porphyrin. The binding Co-N-O angle and energy barrier for the precession were estimated to be 122.8° and 40 meV, respectively, with a lateral size of 0.18 nm. Our study demonstrated that three-dimensional configurations of small-molecule-porphyrin complexes could be probed at the single molecule level using STM. Our results suggest more research into the cases of metalloporphyrins and metallophthalocyanins reacted with NO and the other small molecules is needed.

FIGURE CAPTIONS

Figure 1. (a) The typical STM image of mixed molecular islands on the Au(111) surface after exposure to 900 L of NO gas. (b) The zoomed-in STM image for the marked area in (a). A molecular unit cell is depicted as a yellow square with a lattice constant **a** = 1.40 ± 0.01 nm. The three representative molecules of CoTPP, H_2TPP and NO-CoTPP are denoted by red, blue and green marks, respectively, in (b). The tunneling conditions for (a) and (b) are I_T = 0.1 nA and V_S = -0.6 eV. (c) A high resolution STM image of NO-CoTPP and H_2TPP. The tunneling conditions are I_T = 0.1 nA and V_S = -0.5 eV. At the center of NO-CoTPPs, bright rings are visible. (d) Surface profiles along with the red and blue lines depicted in (c).

Figure 2. Surface profiles along the lateral directions of square ring structure in NO-CoTPP. (a) A high resolution STM image for NO-CoTPP on Au(111). Square ring structure consists of four bright protrusions. (b) Surface profiles of the square ring structure along the colored lines that pass through the four protrusions in (a). The direction of each surface profile is denoted with A~D and A'~D' in (a). Averaged peak-to-peak distances between neighboring protrusions are 0.18 ± 0.01 nm.

Figure 3. Molecular models (a) for the vertical binding and (b) the tilted binding of NO adsorbed to Co-Porphyrin (CoP) on Au(111) obtained with DFT calculations. The light blue, blue, red, gray, and white spheres indicate Co, N, O, C, and H atoms, respectively. Au atoms were not shown. (c) Calculated energy barrier for a 90° precession of NO on CoP. (inset) The definition of precession angle θ. θ = +45°and -45° means that the projected location of O atom on CoP plane is in the line connecting Co and N atoms of CoP as shown in the inset of (c). Simulated constant-current STM images of NO-CoP on Au(111) (d) with fixed NO and (e) with precessing NO.

STM images were simulated at the filled state bias of -0.6 eV. (f) Simulated surface profiles along the diagonal and lateral directions of the square ring in (e). The profiles correspond to the constant currents at the tip-molecule distances that give the lateral size of about 0.18 nm.

Figure 4. Top and side views of model for the tilted binding of NO adsorbed to Co-tetraphenylporphyrin (CoTPP) on Au(111) obtained with DFT calculations. The light blue, blue, red, gray, and white spheres indicate Co, N, O, C, and H atoms, respectively. Au atoms were not shown. (b) Simulated constant-current STM images of NO-CoTPP on Au(111) with precessing NO.

Figure 5. Fourier transform infra-red spectroscopy results obtained from CoTPP with and without NO exposure. Two additional vibration modes 1680 and 1283 cm^{-1} are visible at the spectrum obtained from CoTPP with NO exposure.

TABLE

Table 1. Calculated NO binding energies ($E_{binding}$ in eV) , Co-N-O angles (*a* in degree), and distances (*d* in Å) of Co-N, N-O, and Au-Co for CoP and CoTPP molecules in various conditions.

		Vacuum	Au(111)	Au(111)+vdW
CoP	$E_{binding}$	-1.81	-1.63	-1.61
	a(Co-N-O)	122.8	122.8	122.2
	d(Co-N)	1.80	1.81	1.82
	d(N-O)	1.19	1.19	1.18
	d(Au-Co)		3.90	3.17
CoTPP	$E_{binding}$	-1.67	-1.68	-1.59
	a(Co-N-O)	122.9	125.0	122.1
	d(Co-N)	1.80	1.79	1.82
	d(N-O)	1.19	1.19	1.19
	d(Au-Co)		5.39	3.29

AUTHOR INFORMATION

Corresponding Author

e-mail : yong.hyun.kim@kaist.ac.kr; sjkahng@korea.ac.kr

Author Contributions

H.K. and Y.H.C. contributed equally to this work.

ACKNOWLEDGMENT

The authors gratefully acknowledge financial support from the National Research Foundation (NRF) of Korea (Grant Nos. 2007-0054038, 2010-0025301, and 2010-0018781). Y.H.C. and Y.−H.K. were supported by the NRF (2012R1A2A2A01046191), the Global Frontier R&D (2011-0031566), and the Institute for Basic Science (IBS) (CA-1201-02) programs. H.K. was supported by a Korea University Grant.

FIGURES

Figure 1

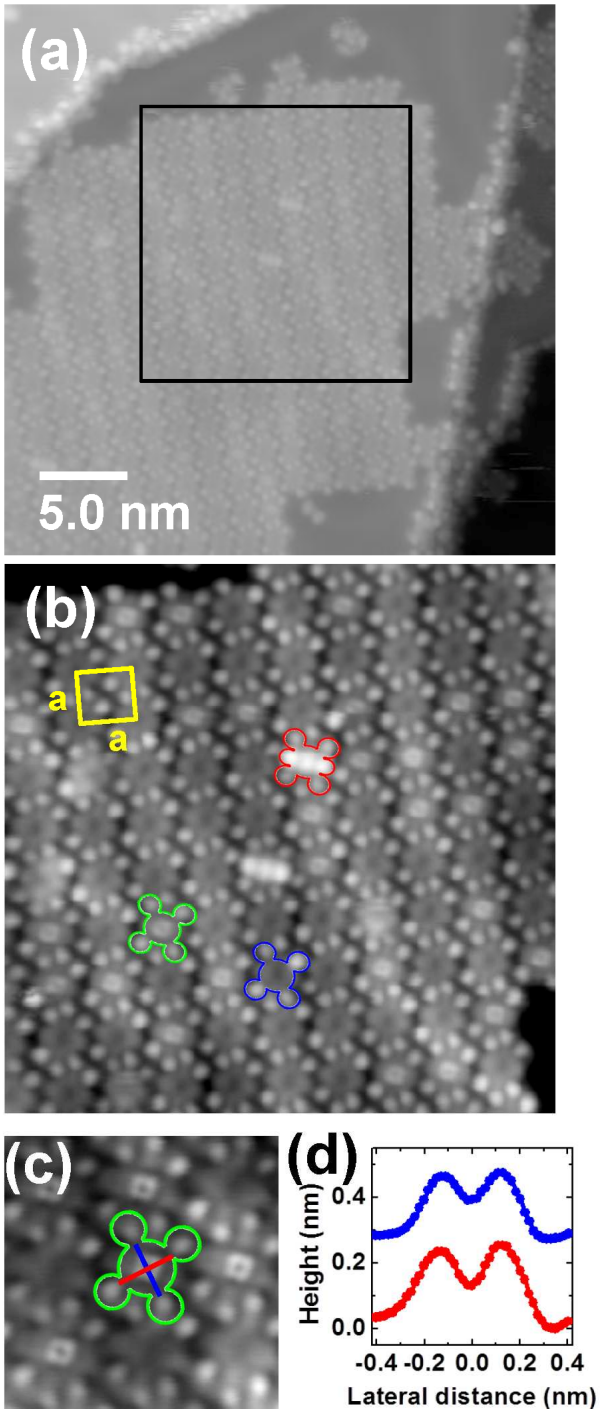

Figure 2

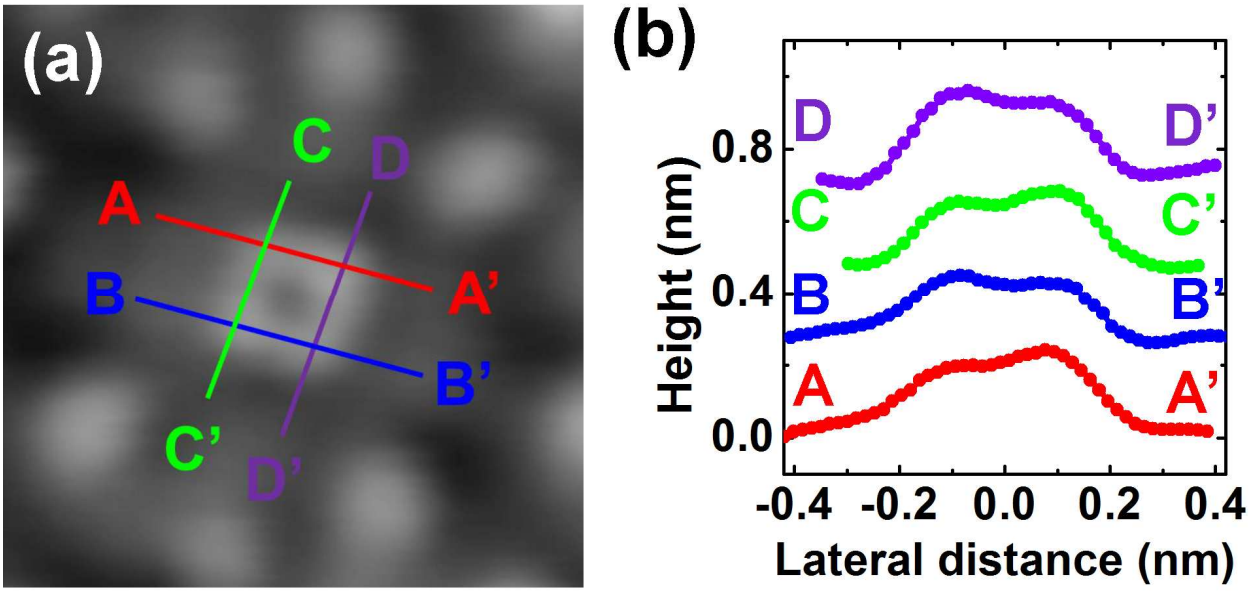

Figure 3

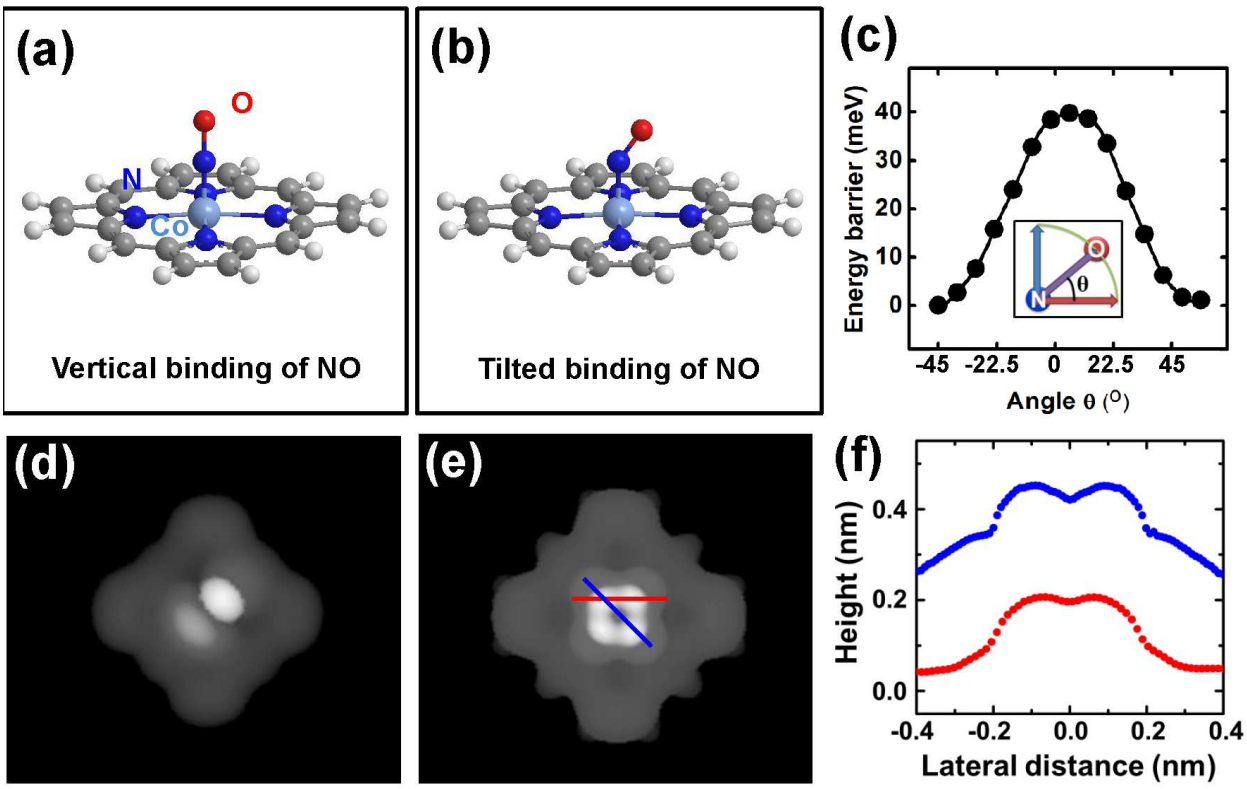

Figure 4

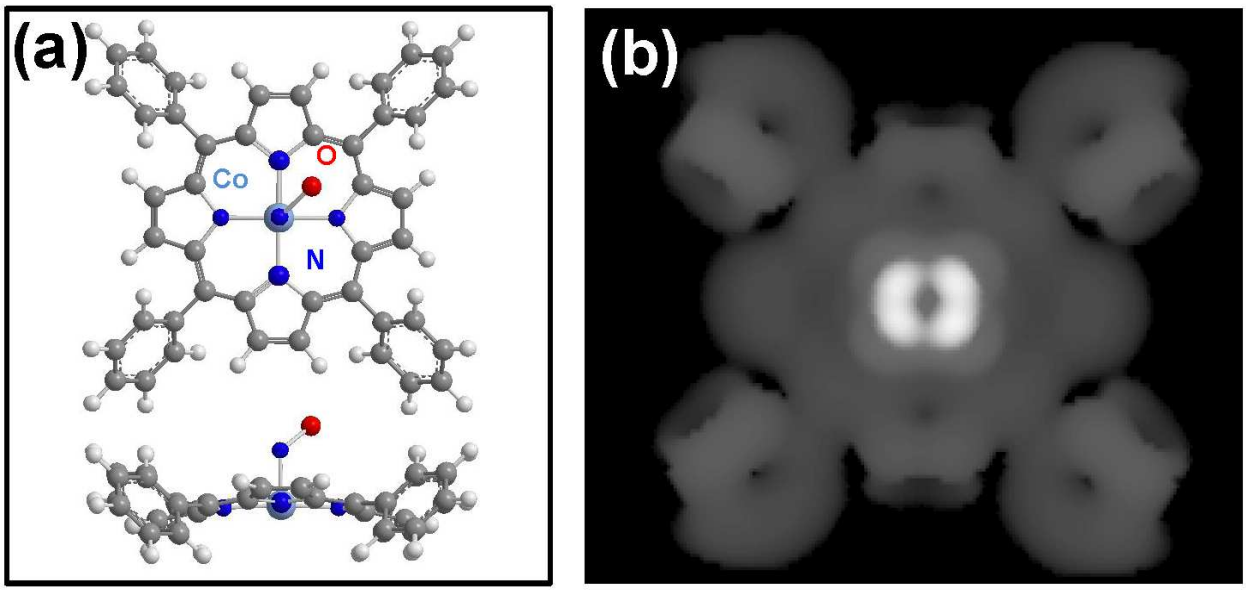

Figure 5

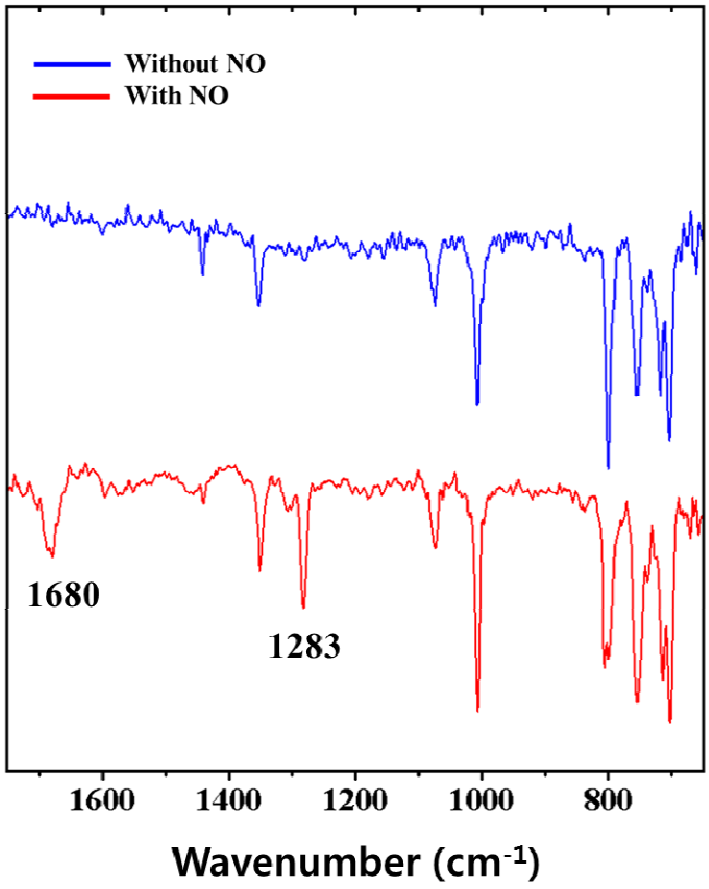

REFERENCES

[1] K. M. Kadish, K. M. Smith, R. Guilard, *The Porphyrin Handbook*, Academic Press, **1999**.
[2] E. Culotta, D. E. Koshland, *Science* **1992**, *258*, 1862-1865.
[3] J. Garthwaite, *Trends Neurosci* **1991**, *14*, 60-67.
[4] C. Griffiths, G. Garthwaite, J. Garthwaite, *Eur J Neurosci* **1998**, *10*, 98-98.
[5] L. Xue, G. Farrugia, S. M. Miller, C. D. Ferris, S. H. Snyder, J. H. Szurszewski, *Proc Natl Acad Sci USA* **2000**, *97*, 1851-1855.
[6] J. P. Collman, R. Boulatov, C. J. Sunderland, L. Fu, *Chem Rev* **2004**, *104*, 561-588.
[7] J. M. C. Ribeiro, J. M. H. Hazzard, R. H. Nussenzveig, D. E. Champagne, F. A. Walker, *Science* **1993**, *260*, 539-541.
[8] N. C. Gerber, I. RodriguezCrespo, C. R. Nishida, P. R. O. deMontellano, *J Biol Chem* **1997**, *272*, 6285-6290.
[9] E. Tsuchida, T. Komatsu, Y. Matsukawa, *Bioconjugate Chem* **2001**, *12*, 71-75.
[10] L. J. Ignarro, *Nitric oxide : biology and pathobiology*, 1st ed., Academic Press, San Diego, **2000**.
[11] F. A. Cotton, G. Wilkinson, C. A. Murillo, M. Bochmann, *Advanced inorganic chemistry*, 6th ed., Wiley-Interscience, **1999**.
[12] J. E. Huheey, E. A. Keiter, R. L. Keiter, *Inorganic Chemistry : Principles of Structure and Reactivity*, 4th ed., Prentice Hall, **1997**.
[13] K. Flechtner, A. Kretschmann, H. P. Steinru□ck, J. M. Gottfried, *J Am Chem Soc* **2007**, *129*, 12110-12111.
[14] C. Wäckerlin, D. Chylarecka, A. Kleibert, K. Mu□ller, C. Iacovita, F. Nolting, T. A. Jung, N. Ballav, *Nat Commun* **2010**, *1*.
[15] W. R. Scheidt, M. K. Ellison, *Acc Chem Res* **1999**, *32*, 350-359.
[16] A. Ghosh, *Acc Chem Res* **2005**, *38*, 943-954.
[17] G. R. A. Wyllie, W. R. Scheidt, *Chem Rev* **2002**, *102*, 1067-1089.
[18] J. A. McCleverty, *Chem Rev* **2004**, *104*, 403-418.
[19] J. H. Enemark, R. D. Feltham, *Coordin Chem Rev* **1974**, *13*, 339-406.
[20] W. R. Scheidt, M. E. Frisse, *J Am Chem Soc* **1975**, *97*, 17-21.
[21] M. K. Ellison, W. R. Scheidt, *J Am Chem Soc* **1997**, *119*, 7404-7405.
[22] M. K. Ellison, W. R. Scheidt, *Inorg Chem* **1998**, *37*, 382-383.
[23] B. L. Westcott, J. H. Enemark, in *Inorganic Electronic Structure and Spectroscopy, Vol. II* (Eds.: A. B. P. Lever, E. I. Solomon), John Wiley and Sons, New York, **1999**, pp. 403-450.
[24] W. R. Scheidt, H. F. Duval, T. J. Neal, M. K. Ellison, *J Am Chem Soc* **2000**, *122*, 4651-4659.
[25] G. R. A. Wyllie, W. R. Scheidt, *Inorg Chem* **2003**, *42*, 4259-4261.
[26] J. L. Hoard, W. R. Scheidt, *J Am Chem Soc* **1973**, *95*, 8281-8288.
[27] G. B. Richter-Addo, S. J. Hodge, G. B. Yi, M. A. Khan, T. Ma, E. Van Caemelbecke, N. Guo, K. M. Kadish, *Inorg Chem* **1996**, *35*, 6530-6538.
[28] L. M. Grande, B. C. Noll, A. G. Oliver, W. R. Scheidt, *Inorg Chem* **2010**, *49*, 6552-6557.
[29] C. J. Groombridge, L. F. Larkworthy, J. Mason, *Inorg Chem* **1993**, *32*, 379-380.
[30] F. Buchner, K. Seufert, W. Auwa□rter, D. Heim, J. V. Barth, K. Flechtner, J. M. Gottfried, H. P. Steinru□ck, H. Marbach, *Acs Nano* **2009**, *3*, 1789-1794.

[31] K. Seufert, W. Auwa□rter, J. V. Barth, *J Am Chem Soc* **2010**, *132*, 18141-18146.
[32] W. Hieringer, K. Flechtner, A. Kretschmann, K. Seufert, W. Auwa□rter, J. V. Barth, A. Go□rling, H.-P. Steinru□ck, J. M. Gottfried, *J Am Chem Soc* **2011**, *133*, 6206-6222.
[33] S. Duhm, A. Gerlach, I. Salzmann, B. Bro□ker, R. L. Johnson, F. Schreiber, N. Koch, *Org Electron* **2008**, *9*, 111-118.
[34] L. Romaner, D. Nabok, P. Puschnig, E. Zojer, C. Ambrosch-Draxl, *New J Phys* **2009**, *11*, 053010.
[35] W. Auwa□rter, K. Seufert, F. Klappenberger, J. Reichert, A. Weber-Bargioni, A. Verdini, D. Cvetko, M. Dell'Angela, L. Floreano, A. Cossaro, G. Bavdek, A. Morgante, A. P. Seitsonen, J. V. Barth, *Phys Rev B* **2010**, *81*, 245403.
[36] L. Scudiero, D. E. Barlow, U. Mazur, K. W. Hipps, *J Am Chem Soc* **2001**, *123*, 4073-4080.
[37] K. Seufert, M. L. Bocquet, W. Auwa□rter, A. Weber-Bargioni, J. Reichert, N. Lorente, J. V. Barth, *Nat Chem* **2011**, *3*, 114-119.
[38] A. Weber-Bargioni, W. Auwa□rter, F. Klappenberger, J. Reichert, S. Lefrancois, T. Strunskus, C. Woll, A. Schiffrin, Y. Pennec, J. V. Barth, *Chemphyschem* **2008**, *9*, 89-94.
[39] H. Kim, W.-j. Son, W. J. Jang, J. K. Yoon, S. Han, S.-J. Kahng, *Phys Rev B* **2009**, *80*, 245402.
[40] L. Scudiero, D. E. Barlow, K. W. Hipps, *The J Phys Chem B* **2000**, *104*, 11899-11905.
[41] G. Kresse, J. Furthmu□ller, *Comp Mater Sci* **1996**, *6*, 15-50.
[42] P. E. Blo□chl, *Phys Rev B* **1994**, *50*, 17953-17979.
[43] J. P. Perdew, K. Burke, M. Ernzerhof, *Phys Rev Lett* **1996**, *77*, 3865-3868.
[44] Y. Y. Sun, Y. H. Kim, K. Lee, S. B. Zhang, *J Chem Phys* **2008**, *129*, 154102.
[45] S. Grimme, *J Comput Chem* **2006**, *27*, 1787-1799.
[46] J. Tersoff, D. R. Hamann, *Phys Rev Lett* **1983**, *50*, 1998-2001.
[47] D. H. Lee, W. J. Lee, W. J. Lee, S. O. Kim, Y.-H. Kim, *Phys Rev Lett* **2011**, *106*, 175502.
[48] G. Henkelman, B. P. Uberuaga, H. Jonsson, *J Chem Phys* **2000**, *113*, 9901-9904.
[49] H. J. Lee, W. Ho, *Science* **1999**, *286*, 1719-1722.
[50] N. Nilius, T. M. Wallis, W. Ho, *J Chem Phys* **2002**, *117*, 10947-10952.
[51] L.-F. Yuan, J. Yang, Q. Li, Q.-S. Zhu, *Phys Rev B* **2001**, *65*, 035415.
[52] H. J. Lee, W. Ho, *Phys Rev B* **2000**, *61*, R16347-R16350.
[53] A. D. Kini, J. Washington, C. P. Kubiak, B. H. Morimoto, *Inorg Chem* **1996**, *35*, 6904-6906.
[54] T. S. Kurtikyan, G. G. Martirosyan, I. M. Lorkovic, P. C. Ford, *J Am Chem Soc* **2002**, *124*, 10124-10129.
[55] I. M. Lorković, P. C. Ford, *Inorg Chem* **2000**, *39*, 632-633.
[56] J. Goodwin, T. Kurtikyan, J. Standard, R. Walsh, B. Zheng, D. Parmley, J. Howard, S. Green, A. Mardyukov, D. E. Przybyla, *Inorg Chem* **2005**, *44*, 2215-2223.

Figure for GRAPHICAL ABSTRACT

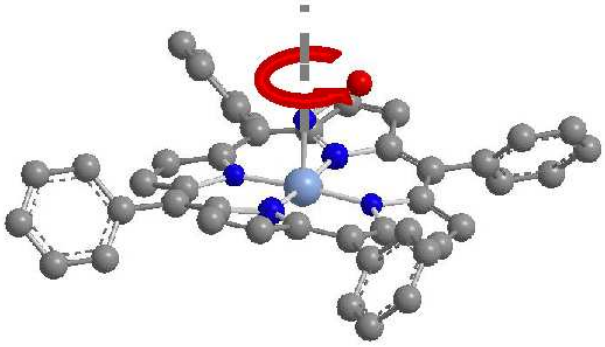

Precessing motion of NO on CoTPP